EQUATIONAL EXPRESSION OF NONLINEAR LOAD-DEFORMATION RELATIONSHIPS OF DOWELLED JOINTS WITH SLOTTED-IN STEEL PLATES AT VARIOUS LATERAL LOADING ANGLES AGAINST THE GRAIN DIRECTION

*Keita Ogawa**

Assistant Professor
E-mail: ogawa.keita@shizuoka.ac.jp

Kenji Kobayashi

Associate Professor
College of Agriculture, Academic Institute, Shizuoka University
Shizuoka, Japan
E-mail: kobayashi.kenji.b@shizuoka.ac.jp

(Received April 2023)

Abstract. When a rotational moment is applied to a dowelled joint with a slotted-in steel plate connecting the beam and the column, the lateral loads at the individual dowels are applied at various angles against the grain direction. To design the joint or analyze its rotational performance, properties at various angles are required. The main objective of this study was to create a simulation method for nonlinear load-displacement relationships at various angles of the loading direction against the grain direction. In this study, lateral loading tests of dowelled joints with slotted-in steel plates at angles of 0°, 15°, 30°, 45°, 60°, 75°, and 90° were conducted. The load-displacement relationship was measured, and the initial stiffness, proportional limit load, and yield load were obtained. When adopting Hankinson's formula for the three characteristics, the values of n were 1.951, 2.052, and 1.912, respectively. The combined use of two empirical formulas (Hankinson's formula and Foschi's formula) was attempted, and the simulation results agreed well with the experimental results, which verified the usefulness of the simulation method proposed in this study.

Keywords: Timber joint, dowelled joint, lateral load, grain direction.

INTRODUCTION

With the increase in eco-friendly approaches in construction areas, interest in large-scale timber buildings has recently increased. A rigid frame structure using a large-dimensional glulam is a well-adopted structural method for large-scale timber buildings. A dowelled joint with a slotted-in steel plate is a popular connection method used in the structure. When a moment acts on a dowelled joint with a slotted-in steel plate, the joint deforms, as shown in Fig 1. The vicinities of the dowels deform. The angle of the deformation direction against the grain direction is particularly noteworthy. As indicated by the red arrows in Fig 1, each dowel embeds to the timber column at various angles against the grain direction. Embedment at various angles has also been observed in other types of dowelled joints with slotted-in steel plates (Guo and Shu 2019; Shu et al 2019; Leng et al 2020; Chen et al 2022).

To design a column-beam dowelled joint with a slotted-in steel plate, the individual lateral resistance at each dowel should be clarified. For obtaining the lateral resistance at various angles against grain direction, Hankinson's equation (1921) is commonly used. According to the design manual edited by the Architectural Institute of Japan (Komatsu 2010), the initial stiffness K_θ and allowable capacity P_θ at the angle θ were represented by the following equations:

$$K = \frac{K_0 K_{90}}{K_0 \sin^2\theta + K_{90} \cos^2\theta} \quad (1)$$

$$P_\theta = \frac{P_0 P_{90}}{P_0 \sin^2\theta + P_{90} \cos^2\theta} \quad (2)$$

* Corresponding author

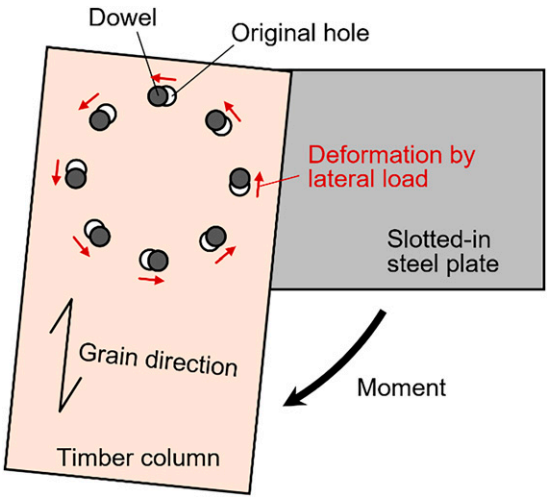

Figure 1. Deformation at the vicinity of dowels when a moment acts on a dowelled joint with slotted-in steel plate.

where K_0 and K_{90} denote the initial stiffness at 0° and 90°, respectively. P_0 and P_{90} are allowable capacities at 0° and 90°, respectively.

To obtain only the characteristics of a column–beam joint, using Eqs 1 and 2, respectively, is enough. On the contrary, there are some cases that need to represent the nonlinear load-deformation relationship of the joint, scientific mechanical analysis of the joint, or precise simulation of the seismic performance of buildings. In these cases, Eqs 1 and 2 are insufficient. Therefore, the authors inferred that an equation representing the nonlinear load-deformation relationship is needed. When investigating past studies on the lateral resistance of dowelled joints with slotted-in steel plates, most of them focused on parallel loads against the grain direction. Although some studies have conducted mechanical tests with perpendicular loading against the grain direction (Kawamoto et al 1992a, 1992b, 1993, Tsujino et al 2001, Gattesco and Toffolo 2004, Uchisako and Tokuda 2009), no precise discussion about the other angles except 0° and 90° was written in these studies. Xu et al (2022) conducted a lateral loading test at an angle of 45° against the grain direction and revealed that the yield load and splitting capacity can be predicted using Johansen's yielding model and the splitting model written in EC5 (EN 1995-1-1 2008). However, stating whether the study sufficiently covered all angles against the grain direction is difficult because the loading test was conducted under limited-angle conditions.

This study conducted the lateral loading test using dowelled joints with a slotted-in steel plate at various angles of the loading direction against the grain direction. The load-deformation relationship and characteristics were clarified. Additionally, equational expressions of the nonlinear load-deformation relationships were attempted using well-known empirical formulas.

MATERIALS AND METHODS

Joint Specimen

A structural glulam made of Japanese cedar (*Cryptomeria japonica* D. Don) was used as the joint specimen. To manufacture the glulam, a lamina with a cross-section size of 30 × 120 mm was prepared. The lamina had a grade of L60 in Japanese Agricultural Standard (2019), which means Young's modulus in bending was 6.0 GPa or over, and the average and lower limit of bending strength were 30 and 22.5 MPa, respectively. Fifteen laminae were adhered, and the size of the glulam was 450 × 120 mm in cross-section and 2000 mm in length. From one glulam, seven specimens were cut such that the angles of the loading direction against the grain direction were 0°, 15°, 30°, 45°, 60°, 75°, and 90°, as shown in Fig 2. The dimensions of the wood pieces were 120 mm × 120 mm × 330 mm. Next, the wood pieces were divided into two pieces, and the size of each piece was 120 mm × 55 mm × 330 mm. Finally, two holes with diameters of 21 mm and one hole with a diameter of 12.5 mm were created, as shown in Fig 2.

The experimental setup for the lateral loading test is illustrated in Fig 3. An 11-mm-thick steel plate (upper in Fig 3) was attached to the crosshead of the testing machine. A pair of wood pieces was connected to the steel plate using two bolts with dimensions of 20 mm. A 62 mm × 62 mm washer was used, and nuts were strongly tightened so that

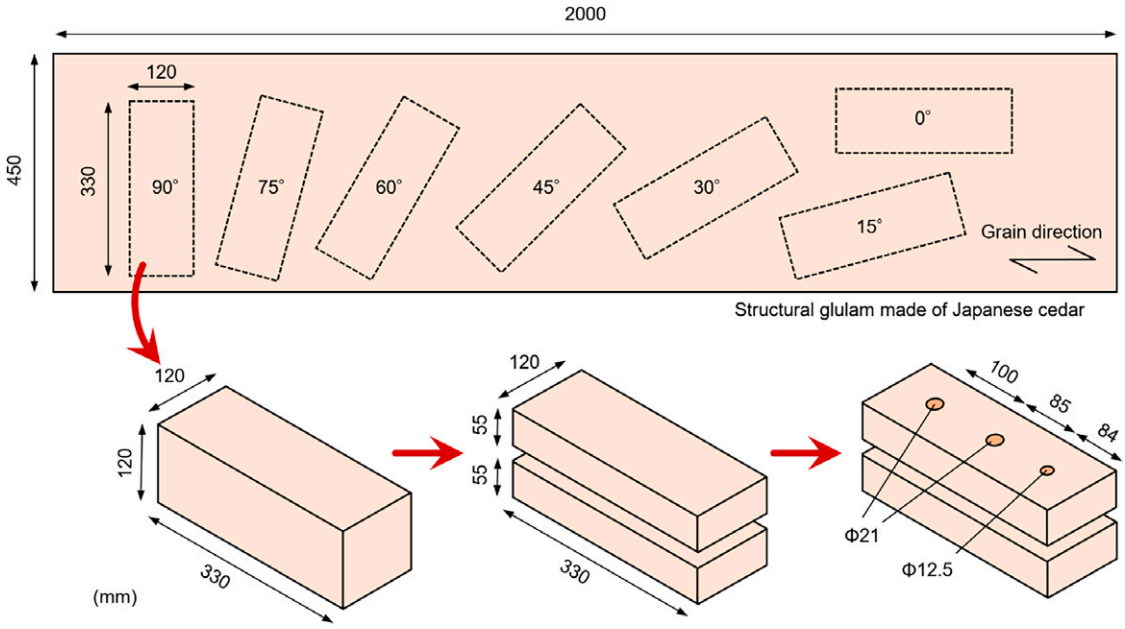

Figure 2. Joint specimen preparation from a structural glulam.

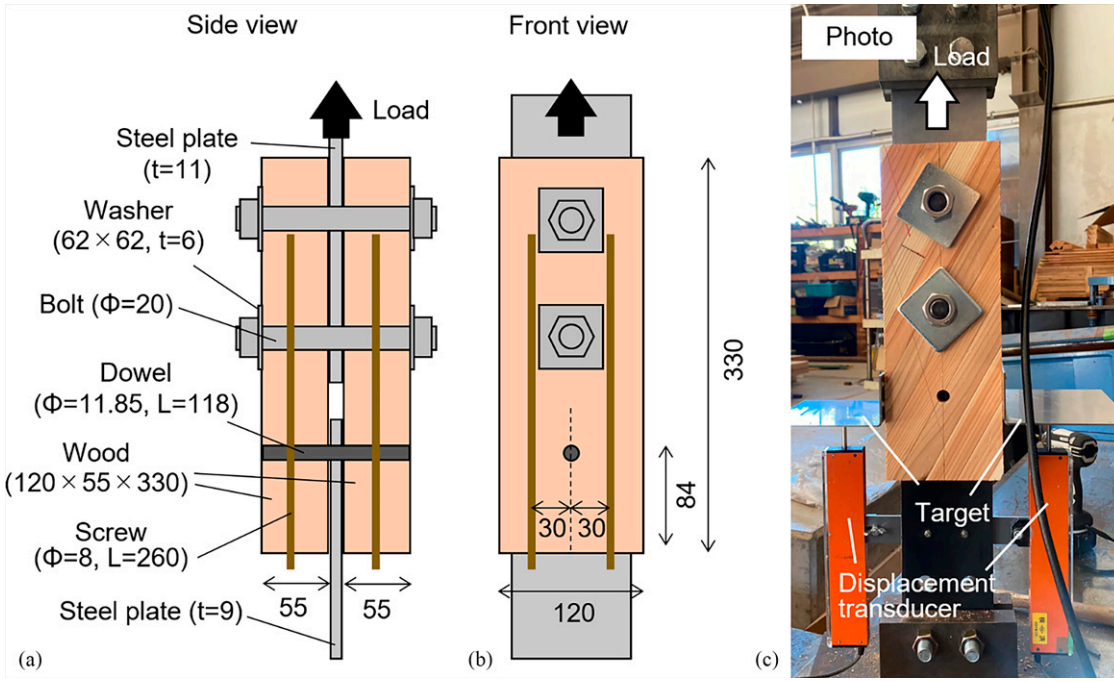

Figure 3. Joint specimen and experimental setup (unit: mm).

each piece was in strong contact with the steel plate. A 9-mm-thick steel plate (lower in Fig 3) was inserted into the gap between the wood pieces. As the thicknesses of the two steel plates were different, there was a gap of 1 mm on each side of the steel plate. Next, a dowel, 11.85 mm in diameter (BX Kaneshin Co., Ltd., Tokyo, Japan, DP-118), was inserted. The distance between the bottom of the wood piece and the dowel was determined to be 84 mm, which was derived using seven times the dowel diameter (Sugimoto and Kawai 2006). The authors conducted the three-point bending test separately to clarify the strength properties of the dowel, and the result revealed that Young's modulus was 168.7 ± 4.9 GPa and yield strength was 600.4 ± 12.6 MPa, respectively (see Appendix). When conducting the lateral loading test using a joint specimen with a loading angle against the grain direction of 15° or more, there is a possibility of crack occurrence along the grain (see Fig 5). Therefore, four screws, 8 mm in diameter and 260 mm in length (Synegic Co., Ltd., Miyagi, Japan, PX8-260), were inserted into the wood pieces to prevent cracks, as shown in Fig 3(a) and (b).

Testing Method

A hydraulic testing machine (Maekawa Testing Machine MFG Co., Ltd., Tokyo, Japan, IPU-B43) was used for the lateral loading tests. A 9-mm-thick steel plate (lower in Fig 3) was connected to the rigid plate, and an 11-mm-thick steel plate (upper in Fig 3) was connected to the crosshead. By moving the crosshead upward, a lateral load was applied to the dowelled joint with a slotted-in steel plate. The loading speed was approximately 2.0 mm/min, and the test was continued until the load decreased by 80% of the maximum value after reaching the maximum load. During the test, the load was measured using a load cell (Tokyo Measuring Instrument Laboratory Co., Ltd., Tokyo, Japan, TCLM-100kNB, capacity:100 kN). To measure the displacement, two displacement transducers (Tokyo Measuring Instrument Laboratory Co., Ltd., SDP-100, capacity:100 mm) were attached to the 9-mm-thick steel plate, and the target was attached to the wood pieces. The average of the read values of the two displacement transducers was adopted as the displacement in this test. The replication of the test was set to six; however, one 90° specimen was fractured during specimen preparation. Therefore, the 90° angle was replicated five times. The average and standard deviation of the density of wood pieces used in the joint specimens were 402.0 ± 21.0 kg/m^3. After the lateral loading test, the MC of the wood pieces was measured with the oven-dry method, and the average and standard deviation was 13.3 ± 0.4%.

RESULTS AND DISCUSSION

Load-Displacement Relationship and Failure Mode

The load-displacement relationships obtained from the lateral loading test are shown in Fig 4. The black line represents the experimental result. In all specimens, the load increased linearly with the increment in displacement at the beginning of loading. When the linear behavior was completed, the slope gradually decreased. The load where the slope decreased was different between the angle conditions; the highest load was observed in the 0° specimens, and the lowest was observed in the 75° or 90° specimens.

Most of the joint specimens maintained their load after yielding, and the load decreased with fracture. The failure modes are shown in Fig 5. In the 0° specimen (Fig 5[a]), shear failure occurred below the dowel hole, as indicated by the blue arrow. When the failure mode of the inside face (in contact with the steel plates) after disassembly of the joint specimen, embedment failure was observed, as shown by the red arrows in Fig 5(a) and (c). As an example of a specimen with the exception of 0°, Fig 5(b) and (c) show the failure observed in the 45° specimen. A crack along the grain occurred after yielding, as indicated by the white arrow, and the load rapidly decreased when the crack occurred. The occurrence of cracks along the grain depends on the crack prevention method, which is not a pure property of dowelled joints with slotted-in steel plates. Therefore, the discussion regarding the maximum load or

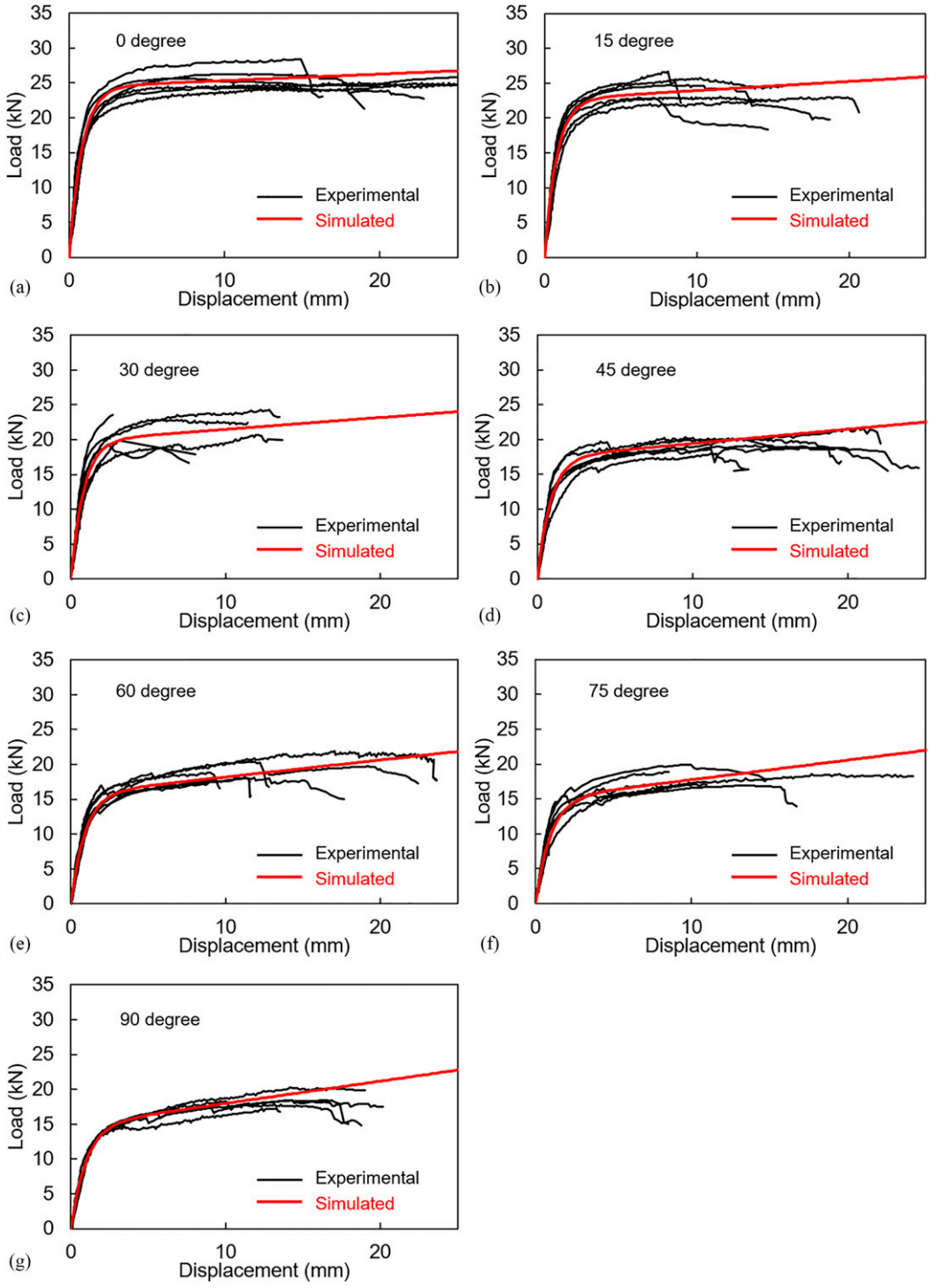

Figure 4. Load–displacement relationships obtained by the lateral loading test. Black lines show the experimental result, and red lines show the simulated result as discussed in the section "Equational Expression of Load–Displacement Relationship".

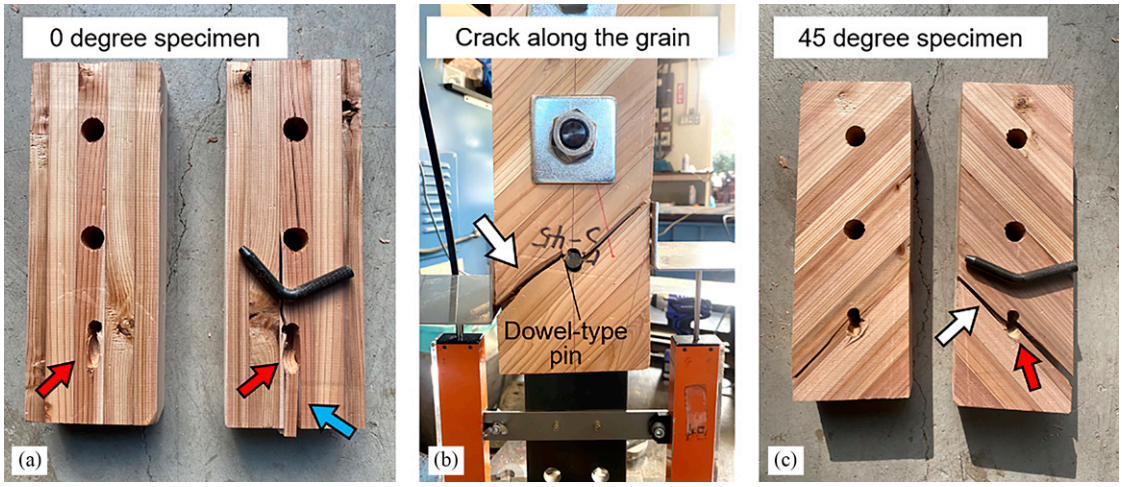

Figure 5. Failure mode. (a) and (c) failure on the inside face (contacted face with steel plates) after disassembly of the joint specimen. (b) The crack occurred along the grain at the end of the loading test. Red, blue, and white arrows indicate embedment deformation, shear failure, and cracks occurring along the grain, respectively.

ultimate load is not appropriate for the load-displacement relationships.

Characteristics

The characteristics were obtained from the load-displacement relationship. The method described in ASTM D5652-21 (2021) was used herein. This method is illustrated in Fig 6. First, a straight line representing linear behavior before yielding was drawn. To draw the line, linear regression for the data plots between $0.1P_{max}$ and $0.4P_{max}$ (where P_{max} indicates the measured maximum load) was conducted, and the initial stiffness K was determined as the slope of the regression line. The proportional limit P_{pl} was determined as the load at which the load-displacement relationship deviated from the linear regression line. Next, a new straight line that was offset from the former line by an amount equal to 5% of the dowel diameter (0.6 mm) was drawn. The yield load P_y was determined as the load at the intersection of the load-displacement and the offset line.

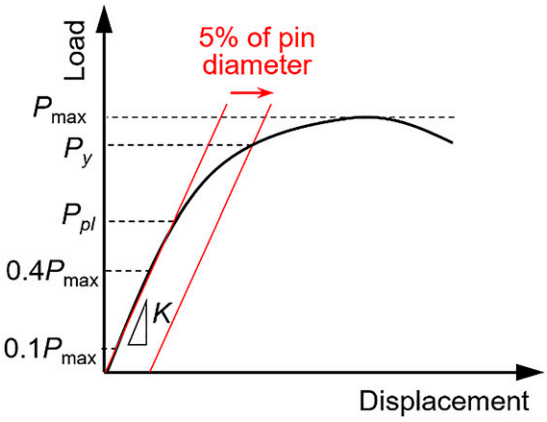

Figure 6. Method for obtaining the characteristics according to ASTM D5652-21.

The characteristics are summarized in Table 1. In all three characteristics, the values tended to decrease with the increment of the angle. For the values of 0° and 15° in the proportional limit load, and 75° and 90° in the yield load, the

Table 1. Characteristics obtained by the lateral test.

Angle (°)	Initial stiffness (kN/mm)		Proportional limit load (kN)		Yield load (kN)	
	Average	SD	Average	SD	Average	SD
0	22.56	4.46	13.12	1.90	20.33	1.81
15	19.07	3.06	13.30	2.42	19.95	1.44
30	18.25	3.59	11.93	2.39	17.78	1.99
45	13.89	2.00	11.11	2.16	15.02	1.89
60	13.37	2.56	10.01	1.82	14.32	1.41
75	12.83	2.40	8.98	1.71	13.30	1.64
90	10.78	2.01	9.23	1.41	13.38	0.58

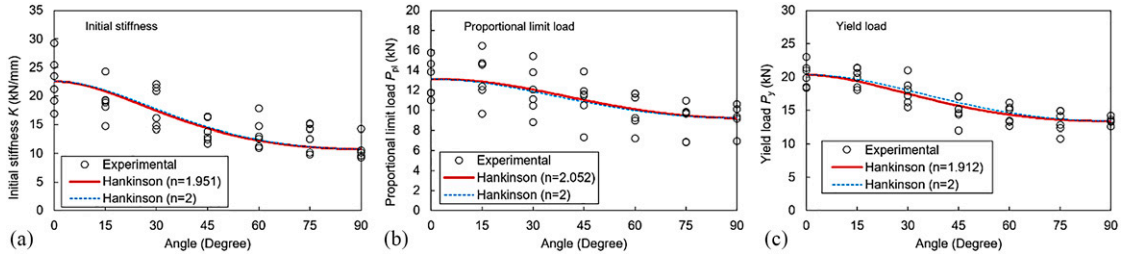

Figure 7. Relationships between angle and characteristics and the result of the adoption of Hankinson's formula.

average of the lower angle was smaller than that of the other. However, the difference was small, and they can be considered as almost the same value.

Hankinson's formula is commonly used to express the characteristics at various angles against the grain direction. Discussing the index of sine and cosine in the denominator was set to 2 (Hankinson 1921). In the literature written by Kollmann and Côtè (1968), the index was replaced with a constant value n, which indicates that the equation was changed to the following:

$$V_\theta = \frac{V_0 V_{90}}{V_0 \sin^n\theta + V_{90}\cos^n\theta} \tag{3}$$

where V_θ, V_0, and V_{90} denote the values of the characteristics at angles of θ, 0°, and 90°, respectively. The constant value n is changed owing to the loading conditions or species. For example, the value of n was between 1.5 and 2.0 in the case of tensile strength parallel to the grain, between 2 and 3 in compression strength parallel to the grain, between 1.8 and 2.3 in bending strength, and 2 in shear strength (Takahashi 1985). As examples of the reports related to timber joints, Chang et al (2006) used $n = 3.1$ for Young's modulus of compression perpendicular to the grain. Schneid and Moraes (2021) conducted an embedment test and reported that the constant value n of embedment strength became 2.0 when using the *Pinus elliottii* sample and 1.5 when using the *Eucalyptus saligna* sample.

For dowelled joints with slotted-in steel plates, the manual (Komatsu 2010) indicates that $n = 2$ for the initial stiffness and allowable capacity, as shown in Eqs 1 and 2. However, there was no clear evidence for $n = 2$. As this study conducted a lateral loading test with various angles against the grain, the values of n for the initial stiffness, proportional limit load, and yield load were validated. First, the values at the angles of 0° and 90° were determined. The average values are listed in Table 1. Next, the value of n was determined using least-squares fitting. As shown in Fig 7, the n values are 1.951, 2.052, and 1.912 for the initial stiffness, proportional limit load, and yield load, respectively. The figure also shows the curve at $n = 2$ with a blue-dashed line. When comparing the red and blue lines, it is almost agreed upon, and it can be considered that $n = 2$ in these three parameters was appropriate.

Equational Expression of Load-Displacement Relationship

To simulate the load-displacement relationship of the joint, this study attempted a combination of two empirical formulas. Foschi's formula is well known to represent the nonlinear behavior of timber joints (Foschi 1974, Foschi and Bonac 1977). The relationship between load P and displacement δ is expressed as follows:

$$P = (m_0 + m_1\delta)\left\{1 - \exp\left(\frac{-k\delta}{m_0}\right)\right\} \tag{4}$$

where k is the initial stiffness, m_1 is the slope of the load-displacement relationship at a large displacement, and m_0 is the intercept of the asymptote with slope m_1. These values were determined by nonlinear least-squares fitting of experimental data. Foschi developed this equation to represent the nonlinear behavior of a nailed joint under lateral loading. Owing to its high versatility, this formula was used to represent various behaviors in

the analyses of timber joints: metal plate joints (Sasaki et al 1988, Gebremedhin et al 1992), and partial compression perpendicular to the grain (Ogawa et al 2016).

As shown in Fig 4, the relationship changed owing to the angle against the grain direction. Here, Eq 4 was fitted to these relationships, and the values of k, m_0, and m_1 were determined. However, the fitting failed at some relationships which fractured soon after yielding (eg three specimens in Fig 4[c]). These specimens were excluded from the following discussion. This study had two initial stiffnesses: K obtained by ASTM D5652-21 (section "Characteristics"), and k in Eq 4. As the methods used to obtain the two were different, this study treated them as having different characteristics. The determined results for the three parameters are shown in the round plots in Fig 8. For the parameters k and m_0, the values decreased with increasing angle (Fig 8[a] and [c]). Then, regression with Hankinson's formula was conducted for the two parameters. The results are as follows:

$$k_\theta = \frac{k_0 k_{90}}{k_0 \sin^{1.996}\theta + k_{90}\cos^{1.996}\theta} \quad (5)$$

$$m_{0-\theta} = \frac{m_{0-0} m_{0-90}}{m_{0-0}\sin^{1.830}\theta + m_{0-90}\cos^{1.830}\theta} \quad (6)$$

where k_θ, k_0, and k_{90} indicate the initial stiffnesses at θ°, 0°, and 90°. The values of k_0 and k_{90} were 29.2 and 15.5 kN/mm, respectively. $m_{0\text{-}\theta}$, $m_{0\text{-}0}$, and $m_{0\text{-}90}$ indicate the values of parameter m_0 at the angle of θ°, 0°, and 90°. The values of $m_{0\text{-}0}$ and $m_{0\text{-}90}$ were 24.6 and 14.8 kN, respectively. As shown in Eqs 5 and 6, the index n was 1.996 for the initial stiffness k and 1.830 for parameter m_0.

With respect to parameter m_1 (Fig 8[b]), the value increases with increasing angle. A similar result was observed in the stress–strain relationship of the wood under partial compression. When partial compression parallel to the grain was applied to a wood specimen, the slope of the load-displacement relationship after the maximum strain was almost zero or negative value (Totsuka et al 2021). In contrast, in the perpendicular direction, the slope after yielding was positive, even if the strain became extremely large (Tanahashi and Suzuki 2020). The reason for the difference seems to be that the stress and strain spread widely and the elastic deformation at the indirectly loaded area (which is called "decay length" in Madsen et al [1982]) occurs in the case of partial compression perpendicular to the grain. A similar mechanism can be adopted to express the behavior observed in Fig 8(b). A linear regression was used to represent the behavior, and the following equation was obtained:

$$m_{1-\theta} = 0.0025\theta + 0.0939 \quad (7)$$

where, $m_{1\text{-}\theta}$ denotes the values of parameter m_1 at the angle of θ°. The coefficient of determination R^2 was obtained as 0.322.

The nonlinear load-displacement relationships at various angle loading directions against the grain direction can be simulated by substituting Eqs 5-7 into Eq 4. The simulated results are shown as red lines in Fig 4. All the red lines agreed well with the experimental results, and the usefulness of the simulation method varied.

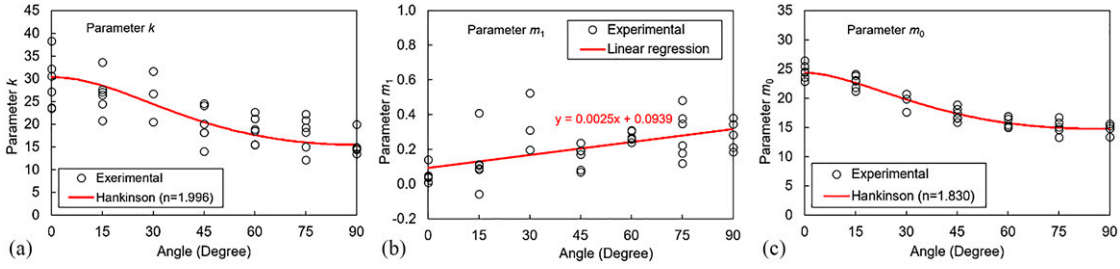

Figure 8. Relationships between angle and parameters in Foschi's equation and the result of adoption of Hankinson's formula.

CONCLUSIONS

In this study, a lateral loading test was conducted using dowelled joint specimens with slotted-in steel plates at various angles of the loading direction against the grain direction. The initial stiffness, proportional limit load, and yield load at various angles were determined, and their values decreased with an increase in angle. When adopting Hankinson's formula for the three characteristics, the values of n were 1.951, 2.052, and 1.912, respectively. The result provided academic evidence for $n = 2$, which is widely used in the design of dowelled joints with slotted-in steel plates. The main objective of this study was to create a simulation method for nonlinear load-displacement relationships at various angles of the loading direction against the grain direction. The combined use of Hankinson's formula and Foschi's formula was adopted, and the simulation results agreed well with the experimental results.

ACKNOWLEDGMENTS

The authors thank Ms. Mamiya, a bachelor's course student at Shizuoka University, for her great help in specimen preparation and test conduction.

REFERENCES

ASTM D5652-21 (2021) Standard test methods for single-bolt connections in wood and wood-based products. West Conshohocken, ASTM, PA.

Chang WS, Hsu MF, Komatsu K (2006) Rotational performance of traditional nuki joints with gap I: Theory and verification. J Wood Sci 52:58-62.

Chen Z, Zhao J, Zhao S, Wang X, Liu H, Zhang L, Xu Q (2022) Experimental study and theoretical analysis on the rotational performance of large-size glulam bolted joints with slotted-in steel plate. Constr Build Mater 341:127785.

EN 1995-1-1:2004+A1:2008 (2008) Eurocode 5: Design of timber structures – Part 1-1: General - Common rules and rules for buildings. European Committee for Standardization, Brussels.

Foschi RO (1974) Load-slip characteristics of nails. Wood Sci 7(1):69-76.

Foschi RO, Bonac T (1977) Load-slip characteristics for connections with common nails. Wood Sci 9(3):118-123.

Gattesco N, Toffolo I (2004) Experimental study on multiple-bolt steel-to-timber tension joints. Mater Struct 37:129-138.

Gebremedhin KG, Jorgensen MC, Woelfel CB (1992) Load-slip characteristics of metal plate connected wood joints tested in tension and shear. Wood Fiber Sci 24(2): 118-132.

Guo JT, Shu Z (2019) Theoretical evaluation of moment resistance for bolted timber connections. Decoration materials, Vol. 303, 3rd International Conference on Building Materials and Materials Engineering (ICBMM 2019). MATEC Web Conference, Lisbon. 03003.

Hankinson RL (1921) Investigation of crushing strength of spruce at carious angle of grain. Air Service Information Circular, Vol. 259. pp. 3-15.

Japanese Agricultural Standard (2019) Japanese Agricultural Standard for Glulam. https://www.maff.go.jp/j/jas/jas_kikaku/attach/pdf/kikaku_itiran2-239.pdf (30 January 2023) (In Japanese).

Kawai N (2006) General testing methods for timber joints. Pages 367-376 *in* Architectural Institute of Japan, ed. Standard for structural design of timber structures. Maruzen, Tokyo (In Japanese).

Kawamoto N, Komatsu K, Kanaya N (1992a) Lateral strength of drift-pin joints in perpendicular to the grain loading I: Effects of edge and end distances on maximum loads. Mokuzai Gakkaishi 38(1):37-45. (In Japanese).

Kawamoto N, Komatsu K, Harada M (1992b) Lateral strength of drift-pin joints in perpendicular to the grain loading II: Effects of test methods on maximum loads. Mokuzai Gakkaishi 38(12):1111-1118. (In Japanese).

Kawamoto N, Komatsu K, Harada M (1993) Lateral strength of drift-pin joints in perpendicular to the grain loading III: Estimation of yield loads by European yield theory. Mokuzai Gakkaishi 39(12):1386-1392. (In Japanese).

Kollmann FFP, Côtè WA (1968) Mechanics and rheology of wood. Pages 292-419 *in* Principles of wood science and technology I solid wood. Springer-Verlag, Berlin.

Komatsu K (2010) Drift pined joints with insert-steel gusset plate. Pages 196-207 *in* Architectural Institute of Japan, ed. Design manual of timber joints. Maruzen, Tokyo (In Japanese).

Leng Y, Xu Q, Harries KA, Chen L, Liu K, Chen X (2020) Experimental study on mechanical properties of laminated bamboo beam-to-column connections. Eng Struct 210:110305.

Madsen B, Hooley RF, Hall CP (1982) A design method for bearing stresses in wood. Can J Civil Eng 9:338-349.

Ogawa K, Sasaki Y, Yamasaki M (2016) Theoretical estimation of the mechanical performance of traditional mortise-tenon joint involving a gap. J Wood Sci 62: 242-250.

Sasaki Y, Miura S, Takemura T (1988) Non-linear analysis of a semi-rigid jointed metal-plate wood-truss. Mokuzai Gakkaishi 34(2):120-125.

Schneid E, Moraes PD (2021) Modification factors of the embedding strength dependent on the temperature and load-to-grain angle for two wood species planted in Brazil. Constr Build Mater 271:121503.

Shu Z, Li Z, Yu X, Zhang J, He M (2019) Rotational performance of glulam bolted joints: Experimental investigation and analytical approach. Constr Build Mater 213:675-695.

Sugimoto K, Kawai N (2006) Dowelled joint. Pages 250-259 *in* Architectural Institute of Japan, ed. Standard for structural design of timber structures. Maruzen, Tokyo (In Japanese).

Takahashi T (1985) Mechanical property. *in* K Nakato, ed. Timber engineering. Yokendo, Tokyo, pp. 206-226. (In Japanese).

Tanahashi H, Suzuki Y (2020) Review on the mechanical models and formulations of embedment of traditional timber joints in Japan. Japan Arch Review 3(2):148-164.

Totsuka M, Jockwer R, Aoki K, Inayama M (2021) Experimental study on partial compression parallel to grain of solid timber. J Wood Sci 67:39.

Tsujino T, Takeuchi N, Kawai T (2001) Collapse loads of drift pin timber joints loaded perpendicular to the grain II. Mokuzai Gakkaishi 47(4):358-363. (In Japanese).

Uchisako T, Tokuda M (2009) Rational timber frame structure jointed with glass fiber reinforced nylon plate I: Basic shear properties of a drift-pin joint to static loads. Mokuzai Gakkaishi 55(4):226-234. (In Japanese).

Xu BH, Liu X, Zhao YH, Bouchaïr (2022) Load-carrying capacity of dowelled joints with slotted-in steel plate loaded at an angle to the grain. Struct 35:350-359.

APPENDIX

The bending properties of the dowel were investigated using a three-point bending test. The experimental setup is illustrated in Fig 9. A universal testing machine (Shimadzu Co., Ltd., AG-I 250 kN) was used for testing.

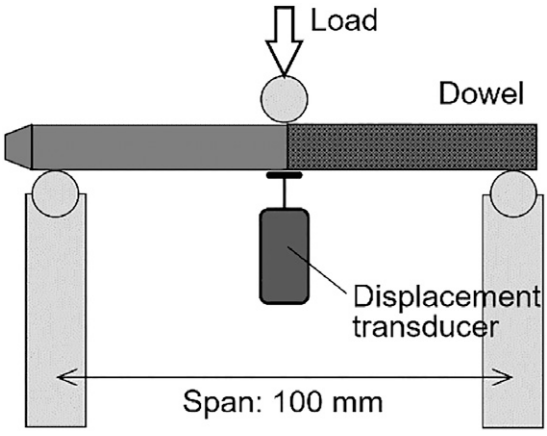

Figure 9. Three-point bending test with the dowel.

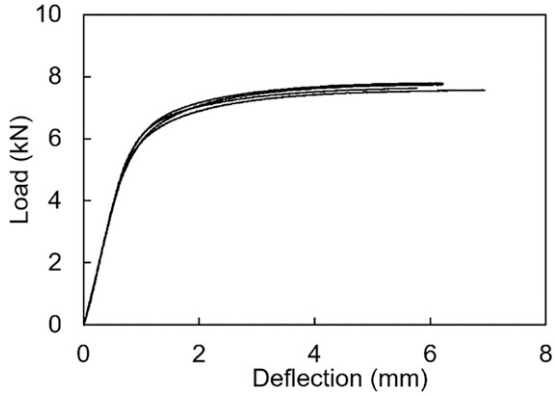

Figure 10. Load–deflection relationship obtained by the bending test with the dowel.

The span L was set to 100 mm. A constant loading ratio of 2.0 mm/min was applied. During the test, the load was measured using a load cell (Shimadzu Co., Ltd., SFL-50kNNAG, capacity: 50 kN), and the deflection at the center of the span was measured using a displacement transducer (Tokyo Measuring Institute Laboratory Co., Ltd., SDP-25, capacity: 25 mm). The bending test was repeated four times. The load-deflection relationships are shown in Fig 10. Young's modulus and yield strength were obtained from these relationships. First, the slope, Δ, at the elastic range was obtained. Here, the slope was obtained by adopting the least-squares method on the data plots in the range of 0.2–0.5 P_{max}, where P_{max} was the maximum load. Using the slope Δ, Young's modulus E_{dowel} was calculated using the following equation:

$$E_{dowel} = \frac{4L^3}{3\pi d^4}\Delta \tag{8}$$

where d denotes the diameter of the dowel (11.85 mm). The yield strength $\sigma_{y\text{-}dowel}$ and the yield load $P_{y\text{-}dowel}$ were determined. According to the standard edited by the Architectural Institute of Japan (Kawai 2006), the method was the same as that for the joint specimen (Fig 6); the load at which a line offset from the straight line fitted to the elastic range of the load-deflection relationship by an amount equal to 5% of the dowel diameter (0.06 mm) intersects the load-deflection relationship. The yield strength $\sigma_{y\text{-}dowel}$ was calculated using the yield load $P_{y\text{-}dowel}$ as the following equation:

$$\sigma_{y-dowel} = \frac{3L}{2d^3}P_{y-dowel} \tag{9}$$